



1 **Role of zooplankton in determining the efficiency of the biological**
2 **carbon pump**

3

4 Cavan, Emma. L. ^{1*}, Henson, Stephanie. A. ², Belcher, Anna. ¹ & Sanders,
5 Richard. ²

6

7 ¹University of Southampton, National Oceanography Centre, European Way,
8 Southampton, SO14 3ZH, UK

9 ²National Oceanography Centre, European Way, Southampton, SO14 3ZH, UK.

10

11 *Corresponding author: Emma L. Cavan, University of Southampton, National
12 Oceanography Centre, European Way, Southampton, SO14 3ZH, UK. (+44)
13 2380 598724. e.cavan@noc.soton.ac.uk.

14

15

16

17

18

19

20

21

22



23 **Abstract**

24 The efficiency of the ocean's biological carbon pump (BCP_{eff} – here the product of particle
25 export and transfer efficiencies) plays a key role in the air-sea partitioning of CO_2 . Despite
26 its importance in the global carbon cycle, the biological processes that control BCP_{eff} are
27 poorly known. We investigate the potential role that zooplankton play in the biological
28 carbon pump using both *in situ* observations and model output. Observed and modelled
29 estimates of fast, slow and total sinking fluxes are presented from three oceanic sites: the
30 Atlantic sector of the Southern Ocean, the temperate North Atlantic and the equatorial Pacific
31 oxygen minimum zone (OMZ). We find that observed particle export efficiency is inversely
32 related to primary production likely due to zooplankton grazing, in direct contrast to the
33 model estimates. The model and observations show strongest agreement in remineralization
34 coefficients and BCP_{eff} at the OMZ site where zooplankton processing of particles in the
35 mesopelagic zone is thought to be low. As the model has limited representation of
36 zooplankton-mediated remineralization processes, we suggest that these results point to the
37 importance of zooplankton in setting BCP_{eff} , including particle grazing and fragmentation,
38 and the effect of diel vertical migration. We suggest that improving parameterizations of
39 zooplankton processes may increase the fidelity of biogeochemical model estimates of the
40 biological carbon pump. Future changes in climate such as the expansion of OMZs may
41 decrease the role of zooplankton in the biological carbon pump globally, hence increasing its
42 efficiency.

43

44 **Keywords**

45 Biological carbon pump, zooplankton, remineralization

46

47



48 1. Introduction

49

50 The biological carbon pump plays an important role in regulating atmospheric carbon dioxide
51 levels (Kwon et al., 2009; Parekh et al., 2006). Phytoplankton in the surface ocean convert
52 inorganic carbon during photosynthesis to particulate organic carbon (POC), a fraction of
53 which is then exported out of the upper ocean. As particles sink through the interior ocean
54 they are subject to remineralization by heterotrophs, such that only a small proportion of
55 surface produced POC reaches the deep ocean (Martin et al. 1987). The efficiency of the
56 biological carbon pump (BCP_{eff} ; defined as the proportion of surface primary production that
57 is transferred to the deep ocean (Buesseler and Boyd, 2009) therefore affects the air-sea
58 partitioning of CO_2 (Kwon et al., 2009). Greater understanding on the controls of this term
59 may consequently result in more accurate assessments of the BCP's role in the global carbon
60 cycle.

61

62 One approach to determine BCP_{eff} over long time scales (millennia) is by assessing the
63 relative proportions of preformed and regenerated nutrients, i.e. the fraction of upwelled
64 nutrients that is removed from surface waters by biological uptake (Hilting et al., 2008).
65 However to assess BCP_{eff} over much shorter timescales (days to weeks) we use the
66 definition of Buesseler & Boyd (2009) where BCP_{eff} is the product of particle export
67 efficiency (PE_{eff} , the ratio of exported flux to mixed layer primary production) and transfer
68 efficiency (TE_{eff} , the ratio of deep flux to exported flux). Using these two parameters together
69 allows a more in-depth analysis of the biological processes involved and thus the assessment
70 of the role of zooplankton in setting BCP_{eff} . Additionally the attenuation coefficients
71 Martin's b (Martin et al. 1987) and the remineralization length scale z^* (Boyd and Trull,



72 2007) are useful to quantify how much exported POC is remineralized in the mesopelagic
73 zone.
74
75 PE_{eff} varies proportionally to primary production, although uncertainty exists as to whether
76 the relationship is inverse or positive (Aksnes and Wassmann, 1993; Cavan et al., 2015;
77 Henson et al., 2015; Laws et al., 2000; Maiti et al., 2013; Le Moigne et al., 2016). Potential
78 controls on PE_{eff} include temperature (Henson et al., 2015; Laws et al., 2000), zooplankton
79 grazing (Cavan et al., 2015), microbial cycling (Le Moigne et al., 2016), mineral ballasting
80 (Armstrong et al., 2002; François et al., 2002; Le Moigne et al., 2012) or large export of
81 dissolved organic carbon (Maiti et al., 2013). Te_{eff} and POC attenuation coefficients describe
82 how much of the exported POC reaches the deep ocean and how much of it is remineralized.
83 Essentially the attenuation of POC with depth is determined by the sinking rates of particles
84 and how rapidly the POC is turned over (Boyd and Trull, 2007). However, these factors
85 themselves are controlled by various other processes such as: ballasting by minerals
86 (François et al., 2002; Le Moigne et al., 2012), epipelagic community structure (Lam et al.,
87 2011), temperature (Marsay et al., 2015), lability of the particles (Keil et al., 2016) and
88 zooplankton diel vertical migration (Cavan et al., 2015). Therefore it is unlikely that any
89 single factor controls BCP_{eff} .
90
91 The role of zooplankton in controlling the efficiency of the BCP is often overlooked, with
92 greater focus on factors such as biominerals for ballasting (De La Rocha and Passow, 2007)
93 or microbial respiration (Herndl and Reinthaler, 2013). Nevertheless zooplankton have the
94 potential to significantly impact the biological carbon pump as they can consume and
95 completely transform particles (Lampitt et al., 1990). Grazing by zooplankton results in POC
96 either passing through the gut and being egested as a fecal pellet, being respired as CO_2 or



97 fragmented into smaller particles through sloppy feeding (Lampitt et al., 1990). Further,
98 zooplankton can undergo diel vertical migration, feeding on particles at night in the surface
99 and egesting them at depth during the day (Wilson et al., 2013). Consequently a significant
100 proportion of POC may escape remineralization in the upper mesopelagic zone (Cavan et al.,
101 2015), where recycling of POC is most intense (Martin et al. 1987).

102

103 In this study we combine observations (made using Marine Snow Catchers, MSCs) and
104 model output to investigate the role of zooplankton in setting the efficiency of the biological
105 carbon pump in three different oceanic regions: the Atlantic sector of the Southern Ocean
106 (SO), the Porcupine Abyssal Plain (PAP) site in the temperate North Atlantic and the
107 Equatorial Tropical North Pacific (ETNP) oxygen minimum zone. The ecosystem model
108 used here, MEDUSA (Yool et al., 2013), was chosen as it separates particle fluxes into slow
109 and fast sinking groups. Additionally the only interactions of zooplankton with particles in
110 MEDUSA are through the production of particles (fecal pellets) and by grazing on slow
111 sinking particles only. Here we compare various indices of BCP_{eff} between the observations
112 and model to infer the role of zooplankton in controlling BCP_{eff} .

113

114 2. Methods

115 2.1 Site description

116 Three very different sites were chosen in this study: the Atlantic sector of the Southern Ocean
117 Ocean (SO, 45 – 65 °S, 20 – 70 °W), the Porcupine Abyssal Plain (PAP) site in the temperate
118 North Atlantic (49 °N, 17 °W) and the Equatorial Tropical North Pacific (ETNP) oxygen
119 minimum zone (13 °N, 91 °W) (Fig. 1). The SO accounts for ~ 20 % of the global ocean CO₂
120 uptake (Park et al., 2010; Takahashi et al., 2002) and is a large high-nutrient-low-chlorophyll
121 region, in part due to limited iron availability (Martin, 1990). Nevertheless, iron from oceanic



122 islands and melting sea ice can cause intense phytoplankton blooms, which may lead to high
123 POC export (Pollard et al., 2009). In the temperate North Atlantic seasonality is high, with
124 phytoplankton blooms occurring in spring and summer (Lampitt et al., 2001). The region
125 contributes disproportionately to global export, accounting for 5 – 18 % of the annual global
126 export (Sanders et al., 2014). In the ETNP region a strong oxygen minimum (OMZ) persists
127 where, between 50 and 1000 m depth, dissolved oxygen concentration can fall below 2 μmol
128 kg^{-1} (Paulmier and Ruiz-Pino, 2009). In OMZs the low oxygen concentrations may lead to a
129 high transfer efficiency of POC flux (Devol and Hartnett, 2001; Hartnett et al., 1998; Keil et
130 al., 2016; Van Mooy et al., 2002).

131

132 2.2 Observations

133 Particles were collected using Marine Snow Catchers (MSCs) (Riley et al., 2012) from the
134 three oceanic sites as shown in Fig. 1. In total 27 stations were sampled, 18 in the SO, 5 at
135 PAP and 4 in the ETNP (Table S1). MSCs have the advantage of being able to separate
136 particles intact into two groups dependent on their sinking rate, fast ($> 20 \text{ m d}^{-1}$) or slow ($<$
137 20 m d^{-1}). MSCs were deployed below the mixed layer depth (MLD), which was determined
138 as the depth with the steepest gradient of salinity and temperature, and usually occurred
139 between 20 and 70 m (Table S1). The shallowest MSC was deployed 10 m below the MLD
140 and another 100 m deeper than this for the Southern Ocean (Cavan et al., 2015) and the PAP
141 site. In the ETNP MSCs were also deployed deeper into the water column to a maximum
142 depth of 220 m.

143

144 Fast and slow sinking particles were collected from the MSC following the protocol by Riley
145 et al. (Riley et al., 2012). Images of fast sinking particles were taken to estimate the
146 equivalent spherical diameter (ESD) of the particles and ESD converted to POC mass *via*



147 conversion factors (Alldredge, 1998; Cavan et al., 2015). Slow sinking and suspended
148 particles were filtered onto ashed (400 °C, overnight) GF/F filters and run in a HNC
149 elemental analyser to determine POC mass. Sinking rates were estimated for fast sinking
150 particles in the SO and at PAP by placing particles into a measuring cylinder filled with *in*
151 *situ* sea water and timing how long it took each particle to pass a discrete point (Cavan et al.,
152 2015). At the ETNP a FlowCAM was used to measure fast particle sinking rates (Bach et al.,
153 2012). All slow sinking particle rates were calculated using the SETCOL method (Bienfang,
154 1981). Fluxes ($\text{mg C m}^{-2} \text{d}^{-1}$) were calculated by dividing the mass of POC (mg) by the area
155 of the MSCs (m^2) and the sinking time of the particles (d) (Cavan et al., 2015). Primary
156 production (PP) was estimated from 8-day satellite-derived data using the Vertically
157 Generalised Productivity Model (Behrenfeld and Falkowski, 1997) applied to MODIS data.

158

159 **2.3 Model output**

160 The ecosystem model MEDUSA (Yool et al., 2013) was used for this study as it distinguishes
161 detrital fluxes in two pools, fast and slow sinking. In MEDUSA, fast sinking particles are
162 assumed to sink more rapidly than the time-step of the model and are remineralized
163 instantaneously at all vertical levels with the flux profile determined by a ballast model
164 (Armstrong et al., 2002). Slow sinking particles sink at 3 m d^{-1} and remineralization is
165 temperature dependent, with zooplankton grazing on slow sinking particles but not on the fast
166 sinking particles. Zooplankton DVM is not parameterised. Primary production is modelled as
167 non-diatom and diatom production, which is summed to give the total depth-integrated
168 primary production. The model was run in hindcast mode at $\frac{1}{4}^\circ$ spatial resolution and output
169 saved with a 5-day temporal resolution. The model output was extracted at the same locations
170 and times as the observations were made and averaged over 12 years (1994 - 2006) to give
171 the climatological seasonal cycle. The model outputs fluxes of particulate organic nitrogen



172 (mg N m⁻² d⁻¹) which are converted to POC (mg C m⁻² d⁻¹) using the Redfield ratio (Redfield,
173 1934).

174

175 **2.4 Data manipulation**

176 For both the observations and the model output the fast and slow sinking fluxes were
177 summed to calculate the total sinking POC flux. Model output was available at fixed depths
178 of 100 and 200 m, which introduces an offset with our at-sea observations (Table S1). This
179 study is therefore assessing BCP_{eff} in the upper ocean only. Parameters calculated to test the
180 efficiency of the biological carbon pump were the percentage contribution of fast and slow
181 sinking particles to the total sinking flux, particle export efficiency (PE_{eff}), the attenuation of
182 flux with depth expressed as b and z^* and transfer efficiency (Te_{eff}).

183

184 PE_{eff} is the proportion of surface produced primary production (PP) that is exported out of
185 the mixed layer (observations) or at 100 m (model) and is calculated by dividing the exported
186 flux by PP. To estimate the attenuation of flux over the upper mesopelagic zone the
187 exponents b (Martin et al. 1987) and z^* (Buesseler and Boyd, 2009) were calculated, where
188 fluxes at the export depth and 100 m below were used for observations and fluxes at 100 and
189 200 m from the model. The b exponent is dimensionless and generally ranges from 0 to 1.5
190 with low values indicating low attenuation, thus low remineralization, and higher values
191 representing high attenuation and remineralization. The z^* (m) exponent is the
192 remineralization length scale, or the depth by which only 37 % of the reference flux (here at
193 the export depth) remains. Thus a large z^* suggests low attenuation and low remineralization
194 of the particle flux. The Te_{eff} is another parameter that represents how much flux reaches the
195 deeper ocean and hence is not remineralized. This is simply calculated by dividing the deep
196 flux (125 – 220 m in observations and 200 m in model) by the export flux. All indices are



197 dimensionless apart from the proportion of slow and fast sinking flux which is expressed as a
198 percentage and z^* which is in metres.

199

200 **3. Results and Discussion**

201 **3.1 Comparison of fluxes**

202 We compare model output with satellite-derived estimates of primary production (PP) POC
203 export and deep (150 - 300 m) fluxes in the upper ocean (Fig. S1). Overall, modelled PP
204 compares well compared to satellite-derived estimates with a strong positive correlation
205 between the two ($p < 0.001$, $r^2 = 0.84$, Fig. S1 a), although the model slightly overestimates
206 PP. When comparing the total sinking export fluxes and total deep fluxes, most points lie
207 below the 1:1 line, suggesting that the model is overestimating POC flux (Figs. S1 b & c).

208

209 **3.2 Export production**

210 The traditional view of export production is that as PP increases, so does POC export out of
211 the mixed layer (Laws et al., 2000). However recent analyses from the Southern Ocean (SO)
212 observe the opposite relationship, that an inverse relationship between PE_{eff} and PP exists
213 (Cavan et al., 2015; Maiti et al., 2013; Le Moigne et al., 2016). We find that for fast sinking
214 particles the model shows PE_{eff} increases with PP (Fig. 2 a) according to a power law
215 function ($p < 0.001$, $r^2 = 0.6$) while the observations show an inverse relationship (logarithmic
216 function, $p < 0.001$, $r^2 = 0.4$), even when including sites outside of the SO.

217

218 However for the slow sinking particles the model shows an inverse relationship between PP
219 and PE_{eff} , similar to that seen in the observations for the fast sinking particles (power law
220 function, $p < 0.001$, $r^2 = 0.97$, Fig. 2 b). Potential reasons for an inverse relationship between PP
221 and PE_{eff} include the temporal decoupling between primary production and export (Salter et



222 al., 2007), seasonal dynamics of the zooplankton community (Tarling et al., 2004) or grazing
223 by zooplankton (Cavan et al., 2015; Maiti et al., 2013; Le Moigne et al., 2016). As previously
224 mentioned one of the differences between the fast and slow sinking detrital pools in the
225 model is that slow sinking particles are grazed on by zooplankton and fast sinking are not.
226 Thus when zooplankton graze on particles in the model an inverse relationship between PE_{eff}
227 and PP exists and when zooplankton grazing is not accounted for, the opposite occurs. This
228 highlights the importance of zooplankton in determining the efficiency of the BCP.

229

230 The observed slow sinking PE_{eff} were generally very low (< 0.05) and thus had little
231 influence on the PE_{eff} for total sinking POC flux, which also had a non-linear inverse
232 relationship with PP ($p < 0.001$, $r^2 = 0.4$, Fig. 2 c). It is important to note that high values of
233 PP ($> 1000 \text{ mg C m}^{-2} \text{ d}^{-1}$) were only present at PAP, and that the SO had the greatest range of
234 PP, so drives a large part of the inverse relationship. Therefore measuring PE_{eff} in other
235 regions with large PP ranges is fundamental to see if this relationship holds outside the sites
236 from this study.

237

238 3.3 Contribution of fast and slow sinking POC fluxes

239 Particles naturally sink at different rates, with one operational definition being that slow
240 sinking particles sink at $< 20 \text{ m d}^{-1}$ and fast sinking particles at $> 20 \text{ m d}^{-1}$ (Riley et al., 2012).
241 Most sediment traps cannot separately measure fluxes of fast and slow sinking particles and
242 are unlikely to capture much of the slow sinking flux due to their deployment in the lower
243 mesopelagic and bathypelagic zones (Buesseler et al., 2007; Lampitt et al., 2008). Slow
244 sinking particles sink too slowly and are remineralized too quickly to reach the deep ocean
245 unless they are formed there. Hence the MSC is a useful tool to analyse the two sinking
246 fluxes separately.



247

248 In both the model and the observations, the slow sinking flux was consistently smaller than
249 the fast sinking flux and generally only contributed < 40 % of the total flux (Fig. S2).
250 However in the model the proportion of slow sinking flux always decreases with depth (Figs.
251 S2 a-c) whereas observations at the PAP site showed the proportion of slow sinking fluxes
252 increased with depth (Figs. S2 e). Increases in slow sinking particles with depth must be from
253 the fragmentation of larger fast sinking particles either abiotically (Alldredge et al., 1990) or
254 from sloppy feeding by zooplankton (Lampitt et al., 1990). Sloppy feeding results in
255 zooplankton fragmenting particles into smaller particles resulting in a larger surface area to
256 volume ratio increasing colonization by microbes and thus remineralization (Mayor et al.,
257 2014). Zooplankton do not graze on fast sinking particles in the model hence neither sloppy
258 feeding nor abiotic fragmentation are represented (Yool et al., 2013). This likely explains
259 why the contribution of slow sinking particles can only decrease with depth in the model,
260 unlike the observations in which slow sinking particles may increase with depth.

261

262 **3.4 Attenuation of POC with depth**

263 The attenuation of POC through the water column describes how quickly POC fluxes are
264 remineralized, with a high attenuation indicating high POC remineralization. We used the
265 parameters b (Martin et al. 1987) and z^* (Boyd and Trull, 2007) to describe the attenuation of
266 flux with depth. A recent study suggests POC remineralization is temperature dependent
267 (Marsay et al., 2015) hence we compared the attenuation coefficients with temperature.
268 Calculated mean b and z^* values for total (fast + slow) sinking POC from the model were
269 similar at all sites (Figs. 3 a & b) with no correspondence with temperature, even though slow
270 sinking particles are remineralized as a function of temperature in the model. Hence slow
271 sinking b and z^* increase and decrease respectively with temperature (Table S2). The



272 observations (for total sinking particles) show a non-linear relationship with temperature that
273 deviates away from the Marsay et al. (Marsay et al., 2015) regression, such that
274 remineralization increases (high attenuation) at temperatures greater than 13 °C. The
275 variability is much greater in the observations than the model, a feature that is consistent
276 across all indices (3 a & b). Apart from at the ETNP where the model and observations agree,
277 the observations consistently show slower POC attenuation compared to the model. The
278 active transfer of POC to depth *via* diel vertical migration (DVM) of zooplankton (Wilson et
279 al., 2008) may contribute to the observed slower rates of POC attenuation. Cavan et al. 2015
280 showed that high Southern Ocean *b* values were a result of DVM, a process not
281 parameterized in the MEDUSA model. Although active transfer *via* DVM is a complex
282 process that may be difficult to model, it is potentially important to include in
283 biogeochemical models, as it has been shown to account for 27 % of the total flux in the
284 North Atlantic (Hansen and Visser, 2016).

285

286 The strong alignment of the modelled and observed attenuation at the ETNP is likely because
287 of the lack of particle processing by zooplankton, by design in the model and naturally in
288 oxygen minimum zones (OMZs). The daytime depth of vertically migrating zooplankton is
289 reduced in OMZs due to low dissolved oxygen concentrations (Bianchi et al., 2013), which at
290 the ETNP reach $< 2 \mu\text{mol kg}^{-1}$ by 120 m. Further the population of zooplankton below this
291 depth is almost non-existent in OMZs (Wishner et al., 2013) and those that are there feed on
292 particles at the surface, not in the OMZ core (Williams et al., 2014). Thus zooplankton
293 consumption and manipulation of particles is greatly reduced in OMZs and is non-existent in
294 the MEDUSA model.

295

296 **3.5 Efficiency of the biological carbon pump**



297 To calculate BCP_{eff} (proportion of mixed layer primary production found at depth, here 150 -
298 300 m) we replicated the BCP_{eff} plots of Buesseler & Boyd (2009) by plotting PE_{eff} against
299 transfer efficiency (T_{eff}) for fast, slow and total sinking particles (Fig. 4). According to the
300 observations, the SO had the highest total sinking BCP_{eff} at 40 %, similar to the maximum
301 observed by Buesseler & Boyd (2009) in the North Atlantic. The SO observations showed a
302 higher BCP_{eff} than the model by about 10 % across all sinking fluxes (Fig. 4). This
303 difference was largely due to a very high T_{eff} (> 1) estimated from observations, which
304 implies fluxes increased at depth. This could be due to active fluxes by vertically migrating
305 zooplankton, possibly krill (Cavan et al., 2015). Active fluxes could account for high
306 observed T_{eff} in the slow sinking particles, as well as fragmentation of larger particles at
307 depth (Mayor et al., 2014).

308

309 Even though the PAP site had the highest PP, the BCP_{eff} was lowest (< 15 %). There were
310 also large differences (up to 15 %) in the BCP_{eff} between the model and the observations at
311 the PAP site driven by large discrepancies in PE_{eff} . Observations of fast sinking PE_{eff} were
312 much lower than predicted by the model (Fig. 4 a), which we suggest could result from active
313 grazing and fragmentation of fast sinking particles by zooplankton. T_{eff} of fast sinking
314 particles were low and consistent with model predictions, suggesting that active transfer via
315 DVM (not parameterized in the model) plays a relatively minor role at the PAP site.
316 Therefore mineral ballasting (Armstrong et al., 2002), which drives T_{eff} in the model, may be
317 the main driver of T_{eff} at PAP. The modelled and observed slow sinking BCP_{eff} were similar
318 at PAP (~ 1 %) despite a large difference in T_{eff} (Fig. 4 b). Fragmentation of fast to slow
319 sinking particles (not included in the model) at depth could explain the difference in slow
320 sinking T_{eff} .

321



322 Finally the BCP_{eff} for the ETNP is very similar between the model and observations for all
323 sinking fluxes (Fig. 4). The similarity in the BCP_{eff} here echoes the similarity shown for
324 POC attenuation with depth. This reiterates our hypothesis that the model and observations
325 agree on BCP_{eff} only in areas of the global ocean where processing of particles by
326 zooplankton is reduced due to very low dissolved oxygen concentrations.

327

328 4. Conclusions

329 We have used observations and model output from the upper mesopelagic zone in 3
330 contrasting oceanic regions to assess the influence of zooplankton on the efficiency of the
331 biological carbon pump. We separately collected *in situ* fast and slow sinking particles, which
332 are also separated into discrete classes in the MEDUSA model. The model has limited
333 processing of particles by zooplankton with only slow sinking detrital POC being grazed
334 upon.

335

336 Our results highlight the crucial role that zooplankton play in regulating the efficiency of the
337 biological carbon pump through 1) controlling particle export by grazing, 2) fragmenting
338 large, fast sinking particles into smaller, slower sinking particles and 3) active transfer of
339 POC to depth *via* diel vertical migration. Comparisons of the model and observations in an
340 oxygen minimum zone provide strong evidence of the importance of zooplankton in
341 regulating the BCP. Here extremely low dissolved oxygen concentrations at depth reduce the
342 abundance and metabolism of zooplankton in the mid-water column. Thus the ability of
343 zooplankton to degrade or repackage particles is vastly reduced in OMZs, and as such it is
344 here that the model, with limited zooplankton interaction with particles, shows the strongest
345 agreement with observations.

346



347 We recommend that grazing on large, fast sinking particles and the fragmentation of fast to
348 slow sinking particles (either *via* zooplankton or abiotically) is introduced into global
349 biogeochemical models, with the aim of also incorporating active transfer. Future changes in
350 climate such as the expansion of OMZs may decrease the role of zooplankton in the
351 biological carbon pump globally, increasing its efficiency and hence forming a positive
352 climate feedback.

353

354 **Acknowledgements**

355 We would like to thank all participants and crew on cruises JR274, JC087, JC097. Thanks to
356 Annike Moje for running all POC samples in Bremen, Germany. Thanks also to Andrew
357 Yool for providing the MEDUSA model output.

358

359 **References**

360

361 Aksnes, D. and Wassmann, P.: Modeling the significance of zooplankton grazing for export
362 production, *Limnol. Oceanogr.*, 38(5), 978–985, 1993.

363 Alldredge, A.: The carbon, nitrogen and mass content of marine snow as a function of
364 aggregate size, *Deep. Res. I*, 45(4-5), 529–541, 1998.

365 Alldredge, A., Granata, T. C., Gotschalk, C. C. and Dickey, T. D.: The physical strength of
366 marine snow and its implications for particle disaggregation in the ocean, *Limnol. Oceanogr.*,
367 35(November), 1415–1428, doi:10.4319/lo.1990.35.7.1415, 1990.

368 Armstrong, R., Lee, C., Hedges, J., Honjo, S. and Wakeham, S.: A new, mechanistic model
369 for organic carbon fluxes in the ocean based on the quantitative association of POC with
370 ballast minerals, *Deep. Res. II*, 49(1-3), 219–236, 2002.

371 Bach, L. T., Riebesell, U., Sett, S., Febiri, S., Rzepka, P. and Schulz, K. G.: An approach for



372 particle sinking velocity measurements in the 3–400 μm size range and considerations on the
373 effect of temperature on sinking rates., *Mar. Biol.*, 159(8), 1853–1864, doi:10.1007/s00227-
374 012-1945-2, 2012.

375 Behrenfeld, M. J. and Falkowski, P. G.: Photosynthetic rates derived from satellite-based
376 chlorophyll concentration, *Limnol. Oceanogr.*, 42(1), 1–20, 1997.

377 Bianchi, D., Stock, C., Galbraith, E. D. and Sarmiento, J. L.: Diel vertical migration :
378 Ecological controls and impacts on the biological pump in a one-dimensional ocean model,
379 27(February), 1–14, doi:10.1002/gbc.20031, 2013.

380 Bienfang, P.: SETCOL - A technologically simple and reliable method for measuring
381 phtoplankton sinking rates, *Can. J. Fish. Aquat. Sci.*, 38(10), 1289–1294, 1981.

382 Boyd, P. and Trull, T.: Understanding the export of biogenic particles in oceanic waters: Is
383 there consensus?, *Prog. Oceanogr.*, 72(4), 276–312, doi:doi:10.1016/j.pocean.2006.10.007,
384 2007.

385 Buesseler, K. and Boyd, P.: Shedding light on processes that control particle export and flux
386 attenuation in the twilight zone of the open ocean, *Limnol. Oceanogr.*, 54(4), 1210–1232,
387 2009.

388 Buesseler, K., Antia, A. N., Chen, M., Fowler, S. W., Gardner, W. D., Gustafsson, O.,
389 Harada, K., Michaels, A. F., van der Loeff'o, M. R., Sarin, M., Steinberg, D. K. and Trull, T.:
390 An assessment of the use of sediment traps for estimating upper ocean particle fluxes, *J. Mar.*
391 *Res.*, 65(3), 345–416, 2007.

392 Cavan, E. L., Le Moigne, F. A. C., Poulton, A. J., Tarling, G. A., Ward, P., Daniels, C. J.,
393 Fragoso, G. M. and Sanders, R. J.: Attenuation of particulate organic carbon flux in the
394 Scotia Sea, Southern Ocean, is controlled by zooplankton fecal pellets, *Geophys. Res. Lett.*,
395 42(3), 821–830, 2015.

396 Devol, A. H. and Hartnett, H. E.: Role of the oxygen-deficient zone in transfer of organic



- 397 carbon to the deep ocean, *Limnol. Oceanogr.*, 46(7), 1684–1690,
398 doi:10.4319/lo.2001.46.7.1684, 2001.
- 399 François, R., Honjo, S., Krishfield, R. and Manganini, S.: Factors controlling the flux of
400 organic carbon to the bathypelagic zone of the ocean, *Global Biogeochem. Cycles*, 16(4),
401 1087, doi:doi:10.1029/2001GB001722, 2002, 2002.
- 402 Hansen, A. N. and Visser, A. W.: Carbon export by vertically migrating zooplankton: an
403 adaptive behaviour model., *Prepr. Submitt. to Mar. Ecol. Prog. Ser.*, doi:10.1002/lno.10249,
404 2016.
- 405 Hartnett, H. E., Devol, A. H., Keil, R. G., Hedges, J. and Devol, A. H.: Influence of oxygen
406 exposure time on organic carbon preservation in continental margin sediments, *Nature*,
407 391(February), 2–4, 1998.
- 408 Henson, S., Yool, A. and Sanders, R.: Variability in efficiency of particulate organic carbon
409 export: A model study, *Global Biogeochem. Cycles*, 33–45, doi:10.1002/2014GB004965,
410 2015.
- 411 Herndl, G. and Reinthaler, T.: Microbial control of the dark end of the biological pump., *Nat.*
412 *Geosci.*, 6(9), 718–724, doi:10.1038/ngeo1921, 2013.
- 413 Hilting, A. K., Kump, L. R. and Bralower, T. J.: Variations in the oceanic vertical carbon
414 isotope gradient and their implications for the Paleocene-Eocene biological pump,
415 *Paleoceanography*, 23(3), n/a–n/a, doi:10.1029/2007PA001458, 2008.
- 416 Keil, R. G., Neibauer, J., Biladeau, C., van der Elst, K. and Devol, A. H.: A multiproxy
417 approach to understanding the “enhanced” flux of organic matter through the oxygen
418 deficient waters of the Arabian Sea, *Biogeosciences*, 13, 2077–2092, doi:10.5194/bgd-12-
419 17051-2015, 2016.
- 420 Kwon, E., Primeau, F. and Sarmiento, J.: The impact of remineralization depth on the air-sea
421 carbon balance, *Nat. Geosci.*, 2, 630–635, 2009.



- 422 De La Rocha, C. and Passow, U.: Factors influencing the sinking of POC and the efficiency
423 of the biological carbon pump, *Deep Sea Res. Part II Top. Stud. Oceanogr.*, 54(5-7), 639–
424 658, doi:10.1016/j.dsr2.2007.01.004, 2007.
- 425 Lam, P. J., Doney, S. C. and Bishop, J. K. B.: The dynamic ocean biological pump: insights
426 from a global compilation of Particulate Organic Carbon, CaCO₃ and opal concentrations
427 profiles from the mesopelagic., *Global Biogeochem. Cycles*,
428 doi:doi:10.1029/2010GB003868, 2011.
- 429 Lampitt, R., Noji, T. and Bodungen, B.: What happens to zooplankton faecal pellets?
430 Implications for vertical flux, *Mar. Biol.*, 23, 15–23, 1990.
- 431 Lampitt, R., Bett, B., Kiriakoulakis, K., Popova, E., Ragueneau, O., Vangriesheim, A. and
432 Wolff, G. A.: Material supply to the abyssal seafloor in the Northeast Atlantic, *Prog.*
433 *Oceanogr.*, 50(1-4), 27–63, 2001.
- 434 Lampitt, R. S., Boorman, B., Brown, L., Lucas, M., Salter, I., Sanders, R., Saw, K., Seeyave,
435 S., Thomalla, S. J. and Turnewitsch, R.: Particle export from the euphotic zone: Estimates
436 using a novel drifting sediment trap, Th-234 and new production, *Deep. Res. Part I-*
437 *Oceanographic Res. Pap.*, 55(11), 1484–1502, doi:DOI 10.1016/j.dsr.2008.07.002, 2008.
- 438 Laws, E., Falkowski, P. G., Smith, W. O., Ducklow, H. and McCarthy, J. J.: Temperature
439 effects on export production in the open ocean, *Global Biogeochem. Cycles*, 14(4), 1231–
440 1246, 2000.
- 441 Maiti, K., Charette, M. a., Buesseler, K. O. and Kahru, M.: An inverse relationship between
442 production and export efficiency in the Southern Ocean, *Geophys. Res. Lett.*, 40(November
443 2012), doi:10.1002/grl.50219, 2013.
- 444 Marsay, C., Sanders, R., Henson, S., Pabortsava, K., Achterberg, E. and Lampitt, R.:
445 Attenuation of sinking particulate organic carbon flux through the mesopelagic ocean, *Proc.*
446 *Natl. Acad. Sci.*, 12(4), 1089–1094, 2015.



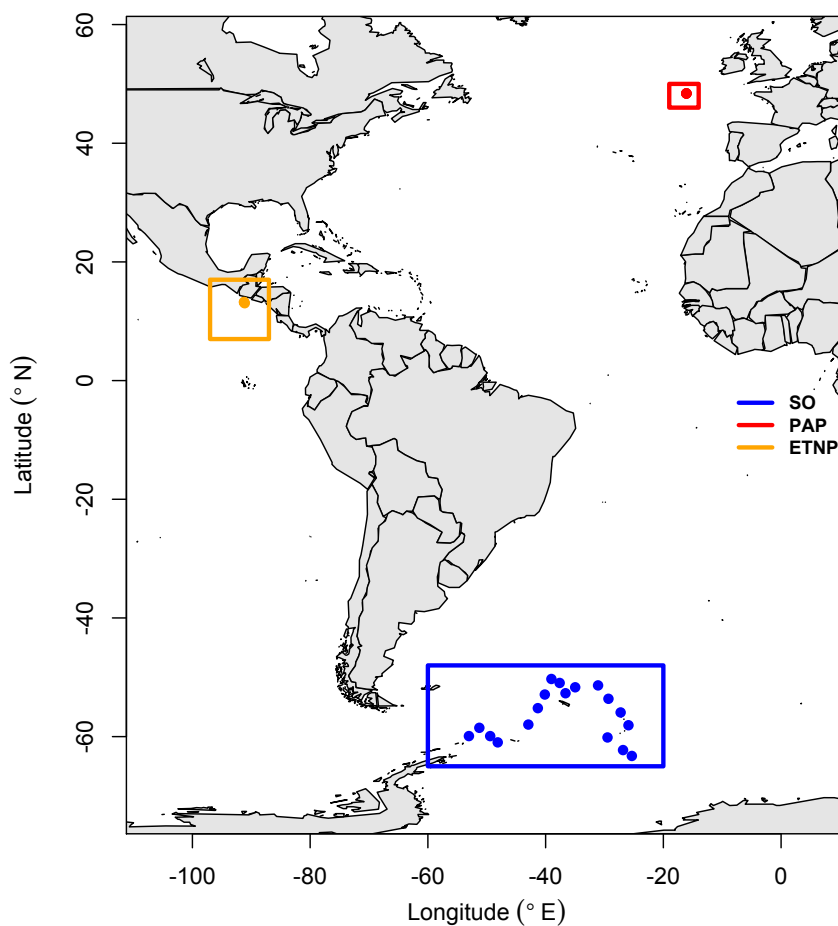
- 447 Martin, J., Knauer, G., Karl, D. and Broenkow, W.: VERTEX: carbon cycling in the north
448 east Pacific, *Deep. Res.*, 34(2), 267–285, 1987.
- 449 Martin, J. H.: Glacial-interglacial CO₂ change: the iron hypothesis,
450 *Paleoceanography/Paleoceanography*, 5(1), 1–13, 1990.
- 451 Mayor, D. J., Sanders, R., Giering, S. L. C. and Anderson, T. R.: Microbial gardening in the
452 ocean's twilight zone, *Bioessays*, 36(12), 1132–7, doi:10.1002/bies.201400100, 2014.
- 453 Le Moigne, F. A. C., Henson, S. A., Cavan, E., Georges, C., Pabortsava, K., Achterberg, E.
454 P., Ceballos-Romero, E., Zubkov, M. and Sanders, R. J.: What causes the inverse relationship
455 between primary production and export efficiency in the Southern Ocean?, *Geophys. Res.*
456 *Lett.*, doi:10.1002/2016GL068480, 2016.
- 457 Le Moigne, F., Sanders, R., Villa-Alfageme, M., Martin, A. P., Pabortsava, K., Planquette,
458 H., Morris, P. and Thomalla, S.: On the proportion of ballast versus non-ballast associated
459 carbon export in the surface ocean, *Geophys. Res. Lett.*, 39(15), doi:10.1029/2012GL052980,
460 2012.
- 461 Van Mooy, B. A. S., Keil, R. G. and Devol, A. H.: Impact of suboxia on sinking particulate
462 organic carbon : Enhanced carbon flux and preferential degradation of amino acids via
463 denitrification, *Geochim. Cosmochim. Acta*, 66(3), 457–465, 2002.
- 464 Parekh, P., Dutkiewicz, S., Follows, M. J. and Ito, T.: Atmospheric carbon dioxide in a less
465 dusty world, *Geophys. Res. Lett.*, 33, doi:10.1029/2005GL025098, 2006.
- 466 Park, J., Oh, I.-S., Kim, H.-C. and Yoo, S.: Variability of SeaWiFs chlorophyll-a in the
467 southwest Atlantic sector of the Southern Ocean: Strong topographic effects and weak
468 seasonality, *Deep Sea Res. Part I Oceanogr. Res. Pap.*, 57(4), 604–620,
469 doi:10.1016/j.dsr.2010.01.004, 2010.
- 470 Paulmier, A. and Ruiz-Pino, D.: Oxygen minimum zones (OMZs) in the modern ocean, *Prog.*
471 *Oceanogr.*, 80(3-4), 113–128, doi:10.1016/j.pocean.2008.08.001, 2009.



472 Pollard, R. T., Salter, I., Sanders, R. J., Lucas, M. I., Moore, C. M., Mills, R. A., Statham, P.
473 J., Allen, J. T., Baker, A. R., Bakker, D. C. E., Charette, M. A., Fielding, S., Fones, G. R.,
474 French, M., Hickman, A. E., Holland, R. J., Hughes, J. A., Jickells, T. D., Lampitt, R. S.,
475 Morris, P. J., Nedelec, F. H., Nielsdottir, M., Planquette, H., Popova, E. E., Poulton, A. J.,
476 Read, J. F., Seeyave, S., Smith, T., Stinchcombe, M., Taylor, S., Thomalla, S., Venables, H.
477 J., Williamson, R. and Zubkov, M. V: Southern Ocean deep-water carbon export enhanced by
478 natural iron fertilization, *Nature*, 457(7229), 577–U81, doi:Doi 10.1038/Nature07716, 2009.
479 Redfield, A. C.: On the proportions of organic derivatives in sea water and their relation to
480 the composition of plankton, University Press of Liverpool., 1934.
481 Riley, J., Sanders, R., Marsay, C., Le Moigne, F., Achterberg, E. and Poulton, A.: The
482 relative contribution of fast and slow sinking particles to ocean carbon export, *Global*
483 *Biogeochem. Cycles*, 26, doi:doi:10.1029/2011GB004085, 2012.
484 Salter, I., Lampitt, R. S., Sanders, R., Poulton, A., Kemp, A. E. S., Boorman, B., Saw, K. and
485 Pearce, R.: Estimating carbon, silica and diatom export from a naturally fertilised
486 phytoplankton bloom in the Southern Ocean using PELAGRA: A novel drifting sediment
487 trap, *Deep. Res. Part II-Topical Stud. Oceanogr.*, 54(18-20), 2233–2259,
488 doi:10.1016/j.dsr2.2007.06.008, 2007.
489 Sanders, R., Henson, S. A., Koski, M., De La Rocha, C. L., Painter, S. C., Poulton, A. J.,
490 Riley, J., Salihoglu, B., Visser, A., Yool, A., Bellerby, R. and Martin, A. P.: The Biological
491 Carbon Pump in the North Atlantic, *Prog. Oceanogr.*, 129, 200–218,
492 doi:10.1016/j.pocean.2014.05.005, 2014.
493 Takahashi, T., Sutherland, S., Sweeney, C., Poisson, A., Metzl, N., Tilbrook, B., Bates, N.,
494 Wanninkhof, R., Feely, R., Sabine, C., Olafsson, J. and Nojiri, Y.: Global sea–air CO₂ flux
495 based on climatological surface ocean pCO₂, and seasonal biological and temperature effects,
496 *Deep Sea Res. Part II Top. Stud. Oceanogr.*, 49(9-10), 1601–1622, doi:10.1016/S0967-



- 497 0645(02)00003-6, 2002.
- 498 Tarling, G. A., Shreeve, R., Ward, P. and Hirst, A.: Life-cycle phenotypic composition and
499 mortality of Calanoides actus in the Scotia Sea; a modeling approach, Mar. Ecol. Prog. Ser.,
500 272, 165–181, 2004.
- 501 Williams, R. L., Wakeham, S., McKinney, R. and Wishner, K. F.: Trophic ecology and
502 vertical patterns of carbon and nitrogen stable isotopes in zooplankton from oxygen
503 minimum zone regions, Deep. Res. Part I Oceanogr. Res. Pap., 90(1), 36–47,
504 doi:10.1016/j.dsr.2014.04.008, 2014.
- 505 Wilson, S., Steinberg, D. and Buesseler, K.: Changes in fecal pellet characteristics with depth
506 as indicators of zooplankton repackaging of particles in the mesopelagic zone of the
507 subtropical and subarctic North Pacific Ocean, Deep. Res. Part II-Topical Stud. Oceanogr.,
508 55(14-15), 1636–1647, doi:10.1016/j.dsr2.2008.04.019, 2008.
- 509 Wilson, S., Ruhl, H. and Smith, K.: Zooplankton fecal pellet flux in the abyssal northeast
510 Pacific : A 15 year time-series study, Limnol. Oceanogr., 58(3), 881–892,
511 doi:10.4319/lo.2013.58.3.0881, 2013.
- 512 Wishner, K. F., Outram, D. M., Seibel, B. a., Daly, K. L. and Williams, R. L.: Zooplankton in
513 the eastern tropical north Pacific: Boundary effects of oxygen minimum zone expansion,
514 Deep Sea Res. Part I Oceanogr. Res. Pap., 79, 122–140, doi:10.1016/j.dsr.2013.05.012, 2013.
- 515 Yool, A., Popova, E. E. and Anderson, T. R.: MEDUSA-2.0: an intermediate complexity
516 biogeochemical model of the marine carbon cycle for climate change and ocean acidification
517 studies, Geosci. Model Dev., 6(5), 1767–1811, doi:10.5194/gmd-6-1767-2013, 2013.



518

519 **Fig. 1.** Map showing study areas. Blue rectangle is location of sites in the Southern Ocean,

520 red is the North Atlantic Porcupine Abyssal Plain and orange the equatorial north Pacific

521 oxygen minimum zone.

522



523

524

525

526

527

528

529

530

531

532

533

534

535

536

537

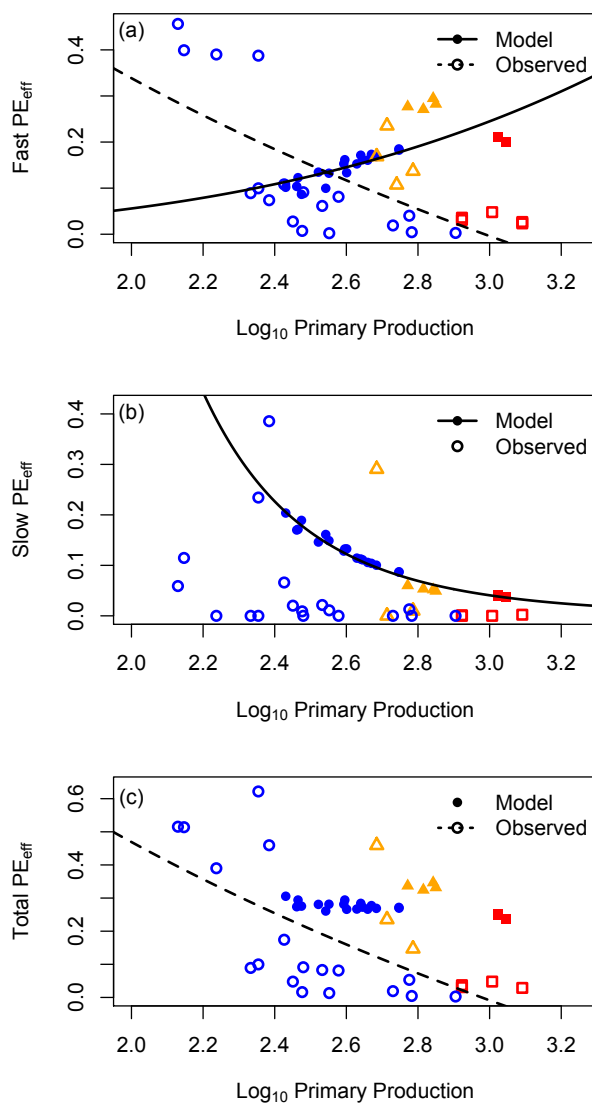
538

539

540

541

542



543

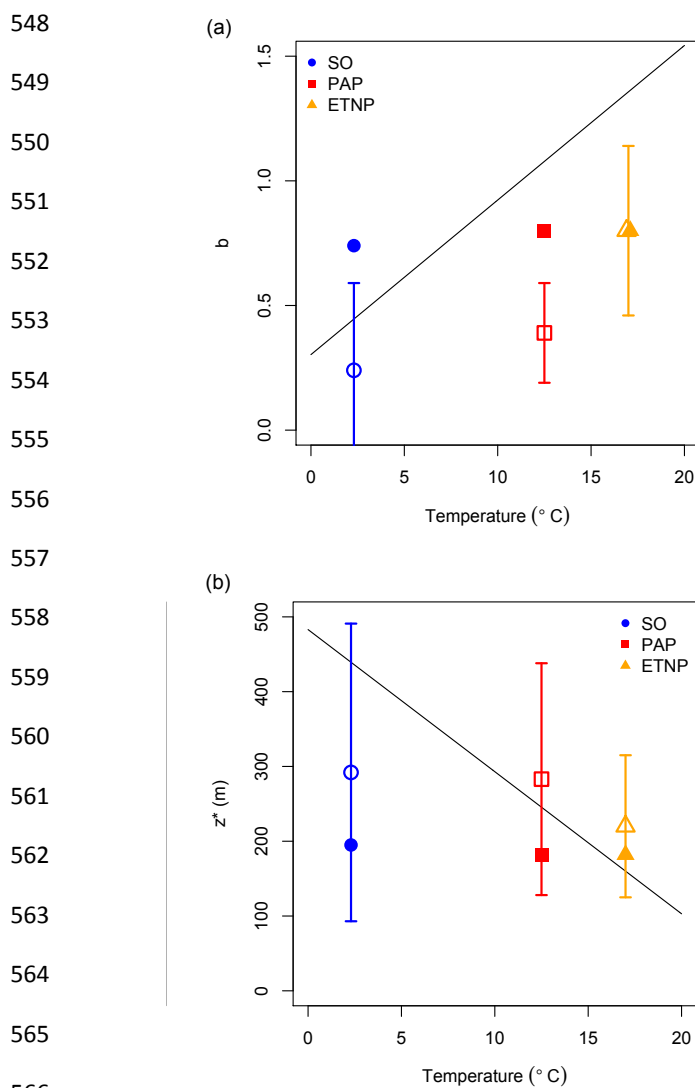
544

545

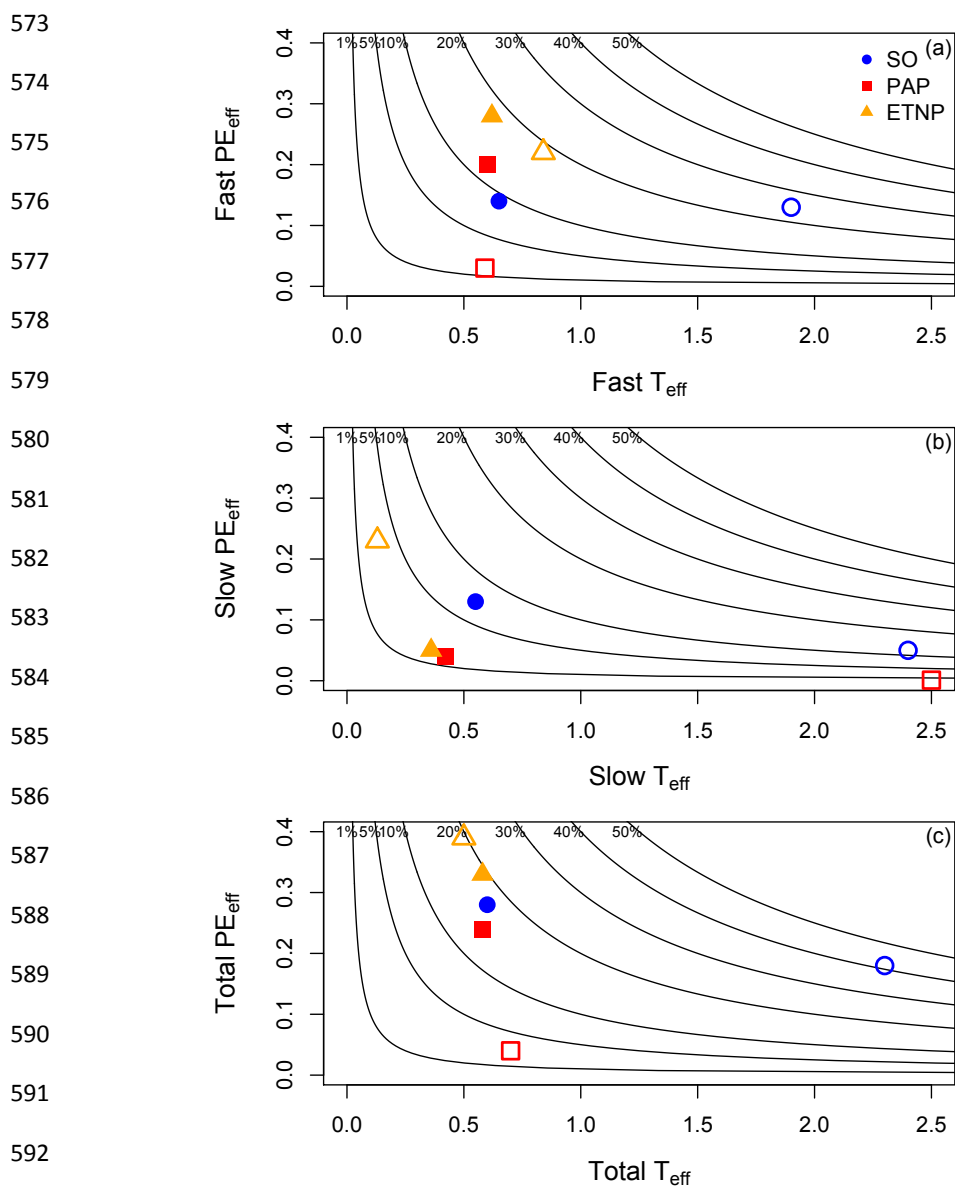
546

547

Fig. 2. Primary production against particle export efficiency (PE_{eff}) for (a) fast sinking, (b) slow sinking and (c) total sinking particles. Blue circles are Southern Ocean, red squares PAP and orange triangles equatorial Pacific. Filled circles and solid black lines show model output and open circles and dashed lines are observations. All fitted lines are statistically significant to at least the 95 % level (see text for details).



567 **Fig. 3.** Total sinking POC attenuation coefficients (a) b and (b) z^* with temperature. Blue
 568 circles are Southern Ocean, red squares PAP and orange triangles equatorial Pacific. Filled
 569 points show model output and open points are observations. Solid line is Marsay et al. (2015)
 570 regression. Error bars are standard error of the mean and only plotted on the observations as
 571 the error is too small in the model. See Table S2 for attenuation coefficients of fast and slow
 572 sinking particles.



593 **Fig. 4.** Efficiency of the biological carbon pump for (a) fast, (b) slow and (c) total sinking
 594 particles. Particle export efficiency (PE_{eff}) is plotted against transfer efficiency (T_{eff}).
 595 Contours represent BCPEff (proportion of primary production at depth). Blue circles are
 596 Southern Ocean, red squares PAP and orange triangles equatorial Pacific. Filled points show
 597 model output and open points are observations.